C. L. Pillmore in (*28*); B. F. Bohor, P. J. Modreski, E. G. Foord, *Science* **236**, 705 (1987).

31. N. L. Carter, C. B. Officer, C. A. Chesner, W. I. Rose, *Geology* **14**, 380 (1986). Shock features have also been recognized in minerals in the Bishop Tuff, California, and the argument currently seems to hinge exclusively on the occurrence of multiple sets of laminae [see discussion in *Geology* **15**, 90 (1987)].
32. A. Rice, *Phys. Earth Planet. Int.* **48**, 167 (1987). According to Rice, peak pressures could have been as high as 1000 kbar, which is more than sufficient for the formation of shocked minerals.
33. W. H. Zoller, J. R. Parrington, J. M. Phelan Kotra, *Science* **222**, 1118 (1983).
34. The modelling calculations of I. Olmez, D. L. Finnegan, and W. H. Zoller [*J. Geophys. Res.* **91**, 653 (1986)] and C. B. Officer *et al.* (*22*) suggest that the Deccan Traps basalts of India, erupted entirely during the magnetic zone embracing the K/T boundary, are of the appropriate volume. See also V. Courtillot and S. Cizowski, *Eos* **68**, 193 (1987).
35. R. Rocchia, D. Broclet, P. Bonte, J. Devineau, C. Jehanno, M. Renard, *Mem. Soc. Geol. Fr.* **150**, (1987), p. 95; J. H. Crocket, C. B. Officer, F. C. Wezel, G. D. Johnson, *Geology*, in press. The fullest data come from the three classic European localities of Gubbio, Stevns Klint, and Caravaca. All suggest that whatever happened increased to a peak at the K/T boundary and then subsided over a period of a few hundred thousand years.
36. M. Tredoux, M. J. de Wit, R. J. Hart, N. M. Lindsay, J. P. F. Sellsehop, "Chemostratigraphy across the Cretaceous-Tertiary boundary at localities in Denmark and New Zealand: "A case for terrestrial origin of the platinum-group element anomaly," *Proc. Internat. Workshop on Cryptoexplosions and Catastrophes in the Geological Record*, Parys, South Africa, 6–10 July 1987.
37. J. H. Crocket *et al.*, in (*35*).
38. N. J. Shackleton, *Palaeogeogr. Palaeoclimatol., Palaeoecol.* **57**, 91 (1986).
39. J. F. Mount, S. V. Margolis, W. Showers, P. Ward, P. Doehne, *Palaios* **1**, 87 (1986).
40. R. B. Koepnick *et al.*, *Chem. Geol.* **58**, 55 (1985); J. Hess, M. L. Bender, J. G. Schilling, *Science* **231**, 979 (1986); H. Elderfield, *Palaeogeogr. Palaeoclimatol. Palaeoecol.* **57**, 71 (1986).
41. R. B. Koepnick *et al. Paleogeogr. Palaeoclimatol. Palaeoecol.* **58**, 55 (1985).
42. After W. V. Sliter, *Init. Rep. Deep-Sea Drill Proj.* **36**, 519 (1976); E. G. Kauffman, in *Treatise on Invertebrate Palaeontology* (Univ. of Kansas Press, Lawrence, 1979), vol. A, p. 418; B. U. Haq, J. Hardenbol, P. R. Vail, *Science* **235**, 1156 (1987). Sliter's curve (Fig. 2A) is based on the amount of continental area covered by sea and is therefore very approximate; it also makes no distinction between different divisions within the stage and merely indicates a progressive Maastrichtian decline correlative with sea-level fall. Kauffman's curve (Fig. 2B), though only a qualitative estimate, is more precise stratigraphically and is based on changes in sedimentary successions as well as areal changes; it indicates a late Maastrichtian sea-level rise followed by a fall to the end of the stage, after a mid-Maastrichtian fall. The revised curve of the Vail group (Fig. 2C), based on seismic stratigraphy, offers even more stratigraphic precision. As with the Kauffman curve, a mid-Maastrichtian fall is followed by an early late Maastrichtian rise, after which there is a rapid and pronounced fall immediately before the end of the stage. Thereafter there is an equally rapid rise, which more or less ceases across the K/T boundary. The claim by Haq *et al.* that the minimum sea level was reached not at but immediately before the end of the period is contested by biostratigraphic work on microfossils [D. S. Jones *et al. Geology* **15**, 311 (1987)]. The Haq *et al.* biostratigraphic database is not available for checking.
43. Deep-Sea Drilling Project Leg 93 to the North Atlantic [J. E. Van Hinte *et al.*, *Geology* **13**, 392, 397 (1985)] and Leg 74 in South Atlantic [P. E. Borella, *Init. Rep. Deep-Sea Drill. Proj.* **74**, 645 (1984)]. Van Hinte *et al.* tentatively relate the turbidite event to an impact-induced tsunami.
44. The one exception to date is the detailed profile at Braggs, Alabama [see Jones *et al.*, in (*42*)]. The rise in ^{87}Sr/^{86}Sr at the K/T boundary tentatively suggests a duration broadly comparable to the kaolinite event at Gubbio.
45. M. J. Johnsson and R. C. Reynolds, *J. Sedim. Petrol.* **56**, 501 (1986).
46. N. L. Carter, C. B. Officer, H. R. Naslund, in preparation. Rare quartz grains with shock lamellae have been found throughout the 4 m section.
47. Walvis Ridge region [H. Chamley, H. Maillot, G. Duee, C. Robert, *Init. Rep. Deep-Sea Drill. Prog.* **74**, 685 (1984)]; Patagonia and Seymour Island (C. Macellari, personal communication); Offshore Drilling Project Leg 113, Weddell Sea [*JOIDES J.* **13**, 13 (June 1987)].
48. S. M. Stanley, *Extinction* (Freeman, New York, 1987).
49. D. Jablonski, in *Causes and Consequences of Mass Extinctions*, D. K. Elliott, Ed. (Wiley, New York, 1986), p. 183.
50. R. B. Stothers, J. A. Wolf, S. Self, M. R. Rampino, *Geophys. Res. Lett.* **13**, 725 (1986).
51. J. A. Crocket *et al.*, in preparation.
52. M. E. Bailey, D. A. Wilkinson, A. W. Wolfendale, *Mon. Not. R. Astron. Soc.* **227**, 863 (1987).
53. W. C. Pitman, *Bull. Geol. Soc. Am.* **89**, 1389 (1978); D. T. Donovan and E. J. W. Jones, *J. Geol. Soc.* **136**, 187 (1979).
54. A. Hallam, *J. Geol. Soc.* **142**, 433 (1985).
55. D. E. Loper and K. McCartney, *Geophys Res. Lett.* **13**, 1525 (1986). A similar correlation of the K/T extinctions with events in the core-mantle boundary layer has more recently been proposed by V. Courtillot and J. Besse [*Science* **237**, 1140 (1987)].
56. P. R. Vogt, *Nature (London)* **240**, 338 (1972).
57. I thank the following for stimulating discussion and helpful comments, though they do not necessarily share the viewpoint presented here: F. Asaro, B. F. Bohor, E. Buffetaut, N. L. Carter, M. J. de Wit, C. L. Drake, W. Goodfellow, D. J. McLaren, L. O. Nicolaysen, C. B. Officer, A. Preisinger, R. C. Reynolds, A. Rice, F. Surlyk, and M. Tredoux. Also I thank N. L. Carter for use of Fig. 3.

Icosahedral Solids: A New Phase of Matter?

PAUL J. STEINHARDT

Numerous examples of metallic alloys have been discovered, the atomic structures of which display an icosahedral symmetry that is impossible for ordinary periodic crystals. Recent experimental results support the hypothesis that the alloys are examples of a new "quasicrystal" phase of solid matter. Observed deviations from an ideal quasicrystal structure can be explained as "phason strains," a special class of defects predicted to be the dominant type of imperfection formed during solidification.

THE DISCOVERY OF SOLIDS WITH ICOSAHEDRAL SYMMETRY (*1*) has led to stimulating debate over the nature of their underlying atomic structure. The electron diffraction patterns of these alloys display sharp peaks, which indicates that the atoms are arranged in a highly ordered lattice, as in crystals; however, the patterns have an icosahedral symmetry that is impossible for periodic crystals (Fig. 1). The icosahedron (Fig. 2) includes fivefold symmetry axes that cannot be incorporated into any periodic, crystalline lattice according to established theorems of crystallography.

The challenge is to find a model for the atomic structure of the alloys that can explain the surprising diffraction pattern as shown in Fig. 1. Perhaps the most radical suggestion has been that the icosahedral solids are examples of "quasicrystals," a hypothetical phase of solid matter with long-range quasiperiodic positional ordering of the atoms in an arrangement with disallowed crystallographic rotational symmetry (*2, 3*). A second proposal, the "icosahedral glass model," assumes that the atoms are frozen in a dense but random arrangement (that is, there is no long-range positional

---

The author is in the Department of Physics, University of Pennsylvania, Philadelphia, PA 19104.

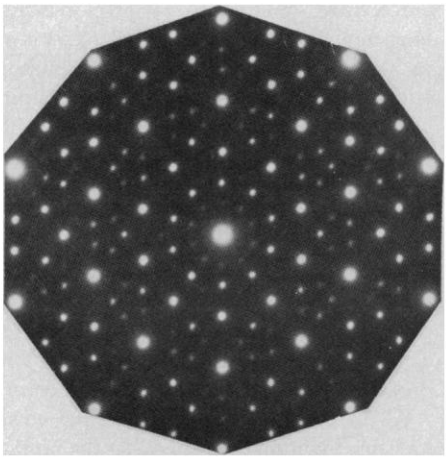

Fig. 1. A diffraction pattern along the fivefold symmetry axis of an icosahedral alloy that displays a symmetry disallowed for crystals [courtesy of P. A. Bancel].

ordering of the atoms) with the constraint that the bonds between neighboring atoms or atomic clusters be oriented along icosahedral symmetry axes (*4, 5*). A third approach uses conventional (periodic) crystalline atomic structures. Although icosahedral symmetry is impossible for a single crystal, many small crystallites may be packed together into an icosahedrally symmetric arrangement, as occurs in "multiple twinning models" (*6*). Alternatively, the symmetry may be approximated by a single crystal with very large atomic clusters that are icosahedrally symmetric and periodically spaced, as occurs in the "large unit cell models."

Whether these new materials represent a new phase of solid matter, as the quasicrystal model suggests, is an issue of enormous significance for physicists, chemists, metallurgists, and crystallographers. A new phase could mean the discovery of materials with physical properties that are fundamentally different from those of previously known solids.

Numerous experimental observations have been made to resolve this issue. The comparison is complicated by the fact that the methods used to solidify the alloys tend to produce strains and defects with respect to the ideal (low-energy) state. Consequently, none of the ideal models is a perfect description of the alloys. Nevertheless, on the basis of many experimental observations, it can be argued that the simplest and most compelling description is the quasicrystal model. The observed imperfections can be explained as "phason strains," a class of elastic distortions of the atomic structure that are predicted by theory to be the dominant type of defect quenched during solidification (*7*).

In this article, the various models and the critical observations that distinguish among them are described. The article is intended to be a brief summary; a more thorough discussion and set of technical references is given in (*8*) and (*9*).

The Central Issue: Long-Range Order

The competing models differ in their predictions of long-range order in the atomic arrangement. Small, well-defined clusters of atoms that repeat throughout the structure exist for each model. The atomic arrangement can be constructed by closely packing these basic structural units (unit cells) in a manner similar to that in which tiles pack to form a mosaic. The long-range order is determined by the arrangement of unit cells in the structure.

In a crystal, all of the unit cells are identical and pack to form a structure with long-range periodic positional order (unit cells are equally spaced along each symmetry direction) and long-range orientational order (unit cells have identical orientations throughout the structure). The orientational order can be characterized by a rotational symmetry, the special set of discrete rotations of the structure that leave the orientations of the unit cells unchanged. According to rigorous theorems of crystallography, periodic positional order is compatible with only twofold, threefold, fourfold, or sixfold axes of rotational symmetry. Icosahedral symmetry is strictly forbidden, since the icosahedron has (six) fivefold symmetry axes. The multiple twinning (*6*) and large unit cell models are both models composed of crystalline constituents with long-range periodic positional order and some allowed crystal orientational symmetry.

Quasicrystals (*2, 3, 8*), like crystals, exhibit long-range positional and orientational order. However, quasicrystals require at least two types of unit cell, and the positional order is quasiperiodic rather than periodic. Quasiperiodic order means that the unit cell positions can be expressed as a sum of periodic functions in which some of the periods are relatively irrational, or incommensurate. An example of a quasicrystal pattern is the Penrose tiling (*10*), shown in Fig. 3A, in which two different unit cells, the acute and obtuse rhombuses, repeat in quasiperiodic sequences along each symmetry direction.

Since quasicrystals are not periodic, their orientational symmetry is not restricted by the usual theorems of crystallography. Quasicrystals can be constructed for any disallowed crystal symmetry (*8*). The Penrose tiling is an example with fivefold orientational symmetry; a completely analogous three-dimensional construction exists for icosahedral symmetry in which oblate and prolate rhombohedra play the same role as the rhombuses do for the Penrose tiling (*2, 8*). Thus, the quasicrystal model predicts long-range quasiperiodic translational order and crystallographically disallowed icosahedral orientational order.

An icosahedral glass (*4, 5, 11*) exhibits long-range icosahedral orientational order, but it does not exhibit long-range positional order. As originally conceived, an icosahedral glass begins with one unit cell that consists of an icosahedral atomic cluster and then grows from this seed by the random packing of additional icosahedral unit cells face-to-face (or in some cases vertex-to-vertex) in such a way that all of the icosahedra have the same orientation. Although long-range icosahedral orientational order is guaranteed by these rules, the randomness of the packing ensures that there is no long-range positional order. An attractive feature of the model is that the growth of such a structure can be accounted for by a simple microscopic picture—the random accretion of icosahedral atomic clusters. In contrast, the quasicrystal model requires more complex atomic interactions to explain the long-range positional ordering.

Diffraction experiments provide quantitative tests of positional and orientational order that can be used to distinguish among the competing models. The critical tests are detailed studies of the relative positions, the widths, and the shapes of the diffraction peaks. If a beam of electrons, neutrons, or x-rays is scattered from an

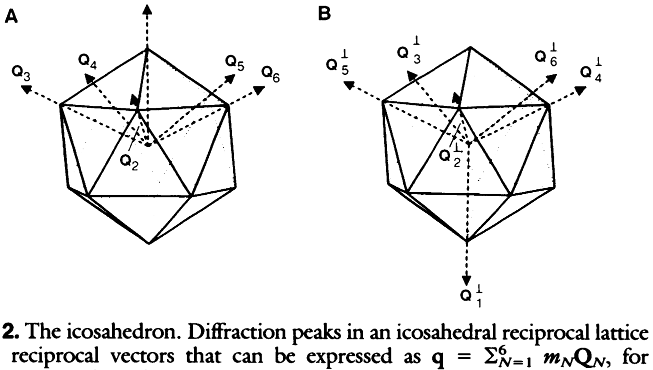

Fig. 2. The icosahedron. Diffraction peaks in an icosahedral reciprocal lattice have reciprocal vectors that can be expressed as $\mathbf{q} = \Sigma_{N=1}^{6} m_N \mathbf{Q}_N$, for integers m_N, where the vectors $\mathbf{Q}_N$ point along the six fivefold symmetry axes shown in (**A**). Each peak can also be assigned a "phason" reciprocal vector, $\mathbf{q}^\perp = \Sigma_{N=1}^{6} m_N \mathbf{Q}_N^\perp$, where the $\mathbf{Q}_N^\perp$ vectors are shown in (**B**).

ordered solid, there are sharp peaks in the scattering intensity as a function of the momentum transferred to the beam. Each diffraction peak can be characterized by a reciprocal vector $\mathbf{q}_i$ which measures the momentum transfer. The vectors $\{\mathbf{q}_i\}$ form a "reciprocal lattice" that has the same orientational symmetry as the atomic structure. Peak positions can be used to determine whether the orientational order is icosahedral or of some allowed crystal rotational symmetry. The diffraction peaks also give information about positional order. If the solid is perfectly ordered, the peaks are perfectly sharp (Bragg diffraction); but, if the solid is somewhat positionally disordered, the peaks will be broadened. In the latter case, the peak shapes and widths can be used to determine the nature of the positional disorder.

The Case Against Conventional Crystallography

Multiple twinning, in which several (periodic) crystallites (called twins) are arranged to form an icosahedral cluster, was the first model considered to explain the icosahedral alloys (*1*). An icosahedrally symmetric reciprocal lattice of diffraction peaks can result by summing the diffraction peaks from each crystallite. Multiple twinning, which involves only conventional (periodic) crystals, is a logical explanation since it is a common, low-energy configuration for crystal growth and since multiple-twinned icosahedral particles have been observed in other materials.

There are so many possible multiple twinning models (for example, those with different crystallite atomic arrangements and symmetries) that an exhaustive computation of the reciprocal lattices and comparison with experiment would not be practical. However, a number of generic tests have been performed that fail to find any direct sign of multiple twinning:

1) High-resolution (atomic-scale) lattice imaging, dark-field imaging, field ion microscopy, and Mössbauer spectroscopy showed no sign of individual crystallites (*1, 12, 13*).

2) Convergent electron beams focused to 15 Å in cross section (through a thickness ≈100 Å) revealed no deviation from icosahedral symmetry as the beam scanned thin samples (*1, 13*). If the sample had contained small crystallites, a convergent beam focusing on just one would have produced a different reciprocal lattice with an allowed crystal symmetry.

3) Diffraction patterns have not shown the streaking characteristic of multiple twinning. Streaks typically appeared in place of sharp peaks because of the slight distortion required to combine crystallites into a cluster with disallowed crystallographic symmetry. (The observed peaks were not perfectly sharp, as described below, but the small distortions in their shapes are quite different from streaking.)

4) X-ray diffraction experiments proved that multiple scattering does not account for the bright diffraction peaks observed in electron diffraction (*14*). In most multiple twinning models of the icosahedral alloys, only a fraction of the bright electron diffraction peaks can be explained by summing the scatterings from each crystallite. Some relatively bright peaks are assumed to occur through multiple scattering; that is, additional peaks can result when electrons scatter several times from different crystallites as they pass through the sample. A method to test for multiple scattering is x-ray scattering. Since x-rays scatter much more weakly than electrons, multiple scattering is diminished and, in fact, is generally not observed in scattering from powders containing many grains. Any peaks added by electron multiple scattering should not be found with x-rays. However, several independent powder x-ray experiments have verified that the bright electron diffraction peaks are also observed in x-ray diffraction.

Recently, Pauling (*6*) has proposed fully detailed multiple twinning models for the icosahedral alloys in which the unit cells are 20 to 30 Å in diameter. These models, however, are subject to the criticisms listed above. In particular, Pauling has pointed out specific bright peaks observed in the electron diffraction patterns that are predicted to be a result of multiple scattering in his model. Yet, these peaks have been clearly observed in several independent powder x-ray experiments. Furthermore, the peak positions computed for the proposed models disagree by as much as 10 standard deviations compared with high-resolution x-ray (synchrotron) measurements (*15*). (Pauling's claim that his model agrees with the observed positions is based on comparison with cruder measurements from electron diffraction photographs.) As a result, the specific models proposed thus far by Pauling have been ruled out.

All of the tests listed above are sensitive enough to rule out multiple twinning provided that the unit cells are comparable in size to those observed in typical metal alloys (<30 Å across). Models in which the unit cell exceeds ≈30 Å can be regarded as "large unit cell models." Such models can only be consistent with the convergent beam experiments [which focus down to a volume $\approx(30\ \text{Å})^3$] if the atomic clusters in the unit cells themselves accurately approximate icosahedral symmetry. In that case multiple twinning becomes an inessential component. By choosing sufficiently large atomic clusters and unit cells, one can always obtain a crystal reciprocal lattice that approximates the observed peak positions to within experimental resolution. If the structure is a single crystal with large unit cells, high-resolution x-ray measurements of peak positions imply that the unit cells must be at least 60 Å across to account for x-ray observations (*15*). Such a unit cell would contain a cluster of more than 15,000 atoms, which vastly exceeds the previous record for similar metallic alloys (≈1000 atoms). Although such a model is a logical possibility, it is generally regarded as quite artificial and, more importantly, lacking in predictive power: the model neither provides a reason why such unusual crystals should form nor does it lead to a prediction of their physical properties.

Quasicrystals Versus Icosahedral Glasses

The distinction between the quasicrystal and icosahedral glass models appears to be quite clear at first glance. An ideal quasicrystal exhibits long-range positional order and hence has a reciprocal lattice of perfectly sharp (Bragg) diffraction peaks. An icosahedral glass is positionally disordered as a result of the random packing of unit cells and has a reciprocal lattice of broadened peaks. However,

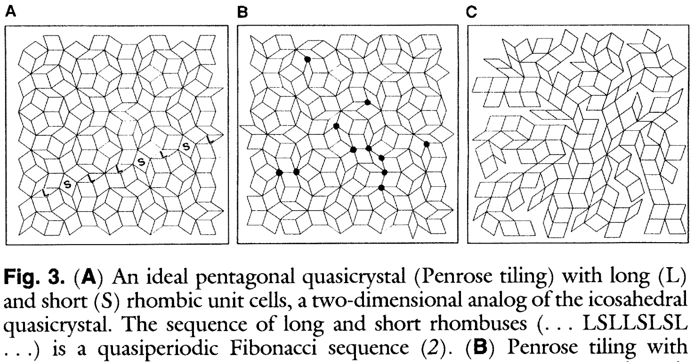

Fig. 3. (**A**) An ideal pentagonal quasicrystal (Penrose tiling) with long (L) and short (S) rhombic unit cells, a two-dimensional analog of the icosahedral quasicrystal. The sequence of long and short rhombuses (. . . LSLLSLSL . . .) is a quasiperiodic Fibonacci sequence (*2*). (**B**) Penrose tiling with smooth, anisotropic (linear) phason strain. Phason strains rearrange the unit cells and produce vertices (marked by black dots) that are disallowed in the original, ideal arrangement in (A). (**C**) Pentagonal glass model, the two-dimensional analog of the icosahedral glass model. Rhombic unit cells are randomly packed. Note the gaps ("rips") induced by the random packing.

quasicrystals grown in the laboratory are not really expected to have perfectly sharp peaks. Microscopic stresses present during solidification will produce small, random distortions (strains) that will disorder the structure and broaden the peaks (*8, 16*).

Theoretical research on the elastic properties of quasicrystals (*17*) suggests that two types of low-energy strain result when a stress is exerted on an ideal quasicrystal: (i) phonon strain, a distortion of the structure obtained by distorting the shapes of the individual unit cells; and (ii) phason strain, a distortion of the structure obtained by rearranging the unit cells (without changing their shape) into a configuration that is disallowed in the ideal (unstrained) configuration (Fig. 3, A and B). Once the solid has grown to macroscopic size and the stresses are removed, phonon strains relax quickly through lattice excitations (phonons) that travel at the speed of sound in the medium. However, phason strains relax by a very slow process [$\geqslant 1$ day (*17*)] in which local atom diffusion rearranges the unit cells back to the ideal (ground-state) configuration. Consequently, "stress-induced phason strains," strains produced by incidental stresses incurred during the growth of a grain, are predicted to be the dominant source of positional disorder in quasicrystals.

Formally, the positional disorder in icosahedral glasses introduced by the random packing of rigid unit cells can be viewed as an extreme form of phason strain (Fig. 3C) (*11, 18*). Compared to an ideal quasicrystal configuration of unit cells, random packing produces roughly one rearrangement per unit cell. Although the two models are actually quite different in character, the fact that both the quasicrystal and icosahedral glass models can lead to the prediction of phason strains suggests that their experimentally distinguishable traits are rather subtle. In fact, by enlarging the size of the unit cell or by adding more packing constraints, one can produce a spectrum of icosahedral glass models with reduced phason strains and sharper diffraction peaks until, ultimately, an ideal quasicrystal is obtained. Furthermore, one can imagine an icosahedral glass that grows with stress-induced phason strains superimposed on the phason strains from the random packing.

The key difference is that the icosahedral glass model leads to a prediction of a component of the phason strain that results from random packing, whereas the quasicrystal model leads a prediction of only incidental stress-induced phason strains. Most importantly, the two forms of phason strain have distinct experimental signatures. First, stress-induced phason strains differ from grain to grain because of varying local stresses during grain growth, whereas the disorder resulting from random packing is "universal," completely determined by the unit cells and packing rules. Second, elasticity theory for quasicrystals suggests that the typical, slowly relaxing phason strains are anisotropic, smoothly varying strains, that include components that grow linearly with distance in some direction (*8, 16*). In contrast, random packing in icosahedral glasses preserves icosahedral symmetry on average and induces strains that vary with distance so sharply that the structure "rips": the unit cells are torn apart so as to produce gaps (occupying up to 55% of the volume) in which no other unit cells can fit (*5, 11*). An underlying assumption is that a mechanism exists for the filling in of the gaps (for example, with amorphous material) simultaneous with the aggregation of icosahedral unit cells. Finally, the diffraction peak shifts, widths, and shapes that result from the two types of phason strain are distinguishable. Each peak in the reciprocal lattice can be characterized by two vectors: the usual reciprocal vector, $\mathbf{q}_i$, and a "phason" reciprocal vector, $\mathbf{q}_i^{\perp}$ (Fig. 2). Stress-induced strains produce peak widths that increase linearly with $|\mathbf{q}_i^{\perp}|$, peak shifts away from the ideal position, $\mathbf{q}_i$, that increase linearly with $|\mathbf{q}_i^{\perp}|$, and asymmetric peak shapes (*16*). The phason strains from random packing in all icosahedral glass models devised thus far produce peak widths that grow quadratically (or, in some cases, more steeply) with $|\mathbf{q}_i^{\perp}|$ (*5, 11, 18*); no systematic peak shifts or asymmetries are expected unless incidental, stress-induced phason strains are superimposed.

Experimental Results Support the Quasicrystal Model

Although a large number of different icosahedral alloys have been discovered (*8, 9*), until recently, systematic studies of the positional disorder from phason strains have been hampered. The problem has been that the icosahedral alloys that were discovered first were less stable than crystalline phases and could only be grown by nonequilibrium methods that led to poor sample quality and small grain sizes (<50 μm across).

Despite these difficulties, several important observations were made. Peak shifts proportional to $|\mathbf{q}_i^{\perp}|$ and anisotropic peak shapes were studied with single-grain electron diffraction and observed to be in accordance with the anisotropic, stress-induced phason strains predicted by the quasicrystal model (*16, 19*). High-resolution (atomic-scale) lattice images obtained by optical Fourier transform of the electron diffraction pattern displayed the characteristic structural distortions expected from gradual, anisotropic phason strains but did not show the inhomogeneity and "rips" predicted by the simplest icosahedral glass models (*20*). X-ray measurements on powders containing many randomly oriented grains of the alloy showed that the peak widths grow monotonically with $|\mathbf{q}_i^{\perp}|$ (*18*). These results are completely consistent with the quasicrystal model with stress-induced, anisotropic phason strains. However, with the exception of the lattice images, the results are also consistent with an icosahedral glass with anisotropic phason strains superimposed on the strains from random packing.

A tremendous breakthrough occurred when two new, icosahedral alloys, $\mathrm{Al_6Li_3Cu}$ (*21, 22*) and, more recently, $\mathrm{GaMg_{2.1}Zn_{3.0}}$ (*23*), were discovered. Both appear to display the same long-range order and, in the case of $\mathrm{Al_6Li_3Cu}$, similar elemental constituents and a similar atomic structure compared to icosahedral alloys discovered previously. However, $\mathrm{Al_6Li_3Cu}$ and $\mathrm{GaMg_{2.1}Zn_{3.0}}$ can be grown by conventional, slow-casting (equilibrium) methods that are used to grow crystals. In fact, $\mathrm{Al_6Li_3Cu}$ and $\mathrm{GaMg_{2.1}Zn_{3.0}}$ appear to be stable (that is, they do not crystallize even when the temperature is raised to near the melting point). This observation already gives indirect support for the quasicrystal model. The quasicrystal phase is expected to be a metastable or stable equilibrium phase, like the crystal phase. In contrast, the icosahedral glass is a phase that is far from equilibrium and that is obtained by rapid aggregation of atoms, similar to ordinary glasses. Such structures are generally unstable and transform irreversibly to other, more ordered states at elevated temperatures (below the melting point).

By carefully controlling the solidification, large single grains of $\mathrm{Al_6Li_3Cu}$ (some greater than 2 cm across) have been grown that can be isolated and individually studied with high-resolution x-ray diffraction (*24, 25*). Finite peak widths were found to be roughly comparable in magnitude to those observed in very rapidly quenched alloys. To some researchers, this suggests that the structural disorder in icosahedral alloys occurs by some "universal" mechanism, one that follows the random packing rules of the icosahedral glass model since disorder remains even with a much slower cooling rate. However, although the solidification rate is slow compared to the rates of methods used to form the original icosahedral alloys, it is not slow enough to remove the disorder induced during the grain growth process. In fact, periodic crystals grown by the same slow methods have been observed to have finite peak widths of nearly the same magnitude (*26*), despite the fact that the disorder relaxation processes in periodic crystals are faster than

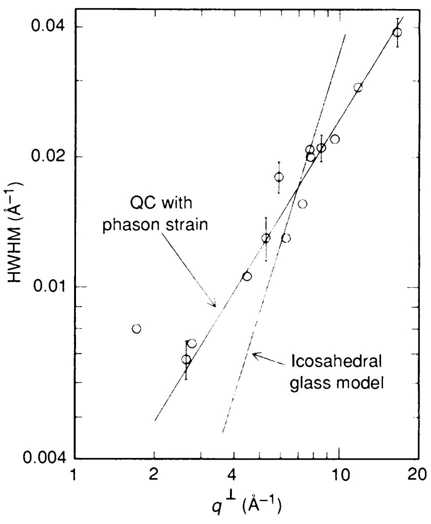

Fig. 4. Log-log plot of peak widths (HWHM; half-width at half-maximum) versus $q^{\perp}$ from single-grain x-ray diffraction of Al_6Li_3Cu [courtesy of P. Horn] (*25*). The slope is sample-independent but the intercept changes from sample to sample. The solid lines illustrate the predictions for the slope of the quasicrystal (QC) and the simplest icosahedral glass models. The systematic dependence on $q^{\perp}$ is not predicted by multiple-twinning models.

those in quasicrystals. More to the point, since the total growth time (<1 hour) is still very short compared with typical phason relaxation times (≫1 day) (*16, 17*), it is natural to expect that the phason strain disorder induced during the quasicrystal growth process should be roughly comparable in magnitude in all of the alloys (although detailed features should vary from sample to sample as a result of uncontrolled variations in growth conditions).

More decisive results for Al_6Li_3Cu have been obtained. First, peak widths (Fig. 4) increase linearly with $|\mathbf{q}_i^{\perp}|$ (*25*), as the quasicrystal model suggests (*16*). Even if stress-induced phason strains are superimposed on the strains resulting from random packing, peak widths are expected to increase quadratically with $|\mathbf{q}_i^{\perp}|$ for large $|\mathbf{q}_i^{\perp}|$ in the icosahedral glass model (*5, 18, 11*). Second, the ratio of the peak width to $|\mathbf{q}_i^{\perp}|$ varies from sample to sample (*25*), which indicates that the disorder is a consequence of incidental stresses during sample growth. Third, the peak shapes are asymmetric and vary in a systematic way with $|\mathbf{q}_i|$ and $|\mathbf{q}_i^{\perp}|$ (*25*). Socolar and Wright (*19*) have shown that the peak asymmetries can be explained in terms of a mosaic of quasicrystal grains with smooth, anisotropic (stress-induced) phason strains which have a very simple mathematical form. The stress-induced phason strains in an icosahedral glass should not be so smooth if there are already sharp variations in the phason strains ("rips") due to random packing. Fourth, closely related atomic models of Al_6Li_3Cu have been constructed corresponding to multiple twinning, icosahedral glass, and quasicrystal packings of identical atomic clusters; the quasicrystal model was found to provide the best fit to the measured radial distribution function (although the icosahedral glass model was only moderately worse) (*27*). (Similar tests have not yet been made for $GaMg_{2.1}Zn_{3.0}$.) Finally, nuggets of both Al_6Li_3Cu and $GaMg_{2.1}Zn_{3.0}$ have been found that exhibit flat facets. The facets in Al_6Li_3Cu form a rhombic triacontahedron (*22, 24, 25*), and the facets in $GaMg_{2.1}Zn_{3.0}$ form a pentagonal dodecahedron (Fig. 5) (*23*), both corresponding to polyhedra with icosahedral symmetry. The facets represent striking evidence of both icosahedral symmetry, including fivefold symmetry axes and long-range positional order. Roughly speaking, facets grow outward by accreting atoms layer by layer; in order to do so, the atoms on one side of a facet must be "aligned" or ordered with respect to atoms on the other side. Faceting is predicted by the quasicrystal model (*28*), but faceting is very difficult to explain if the structure is truly positionally disordered, as occurs in random packing models.

From these observations, one must conclude that the evidence for the random packing predicted by the icosahedral glass model has not been observed in the icosahedral alloys. Nevertheless, the icosahedral glass and the quasicrystal are closely related structurally, and the icosahedral glass model may provide important insights into how quasicrystals grow. The model emphasizes the importance of icosahedral clusters, and evidence for such clusters in both icosahedral and crystalline phases has been observed (*9*). Furthermore, Elser (*11*) has recently shown that, by choosing packing rules so that only special unit cell clusters are energetically preferred and by allowing considerable thermal relaxation (rearrangement) of the unit cells as they are packed together layer by layer, a quasicrystalline structure can result. Apparently the packing energy and the entropy of rearrangement combine to smooth out the phason strains and to produce a structure with sharp (Bragg) diffraction peaks.

Conclusions

Experimental evidence has been obtained that is fully consistent with the quasicrystal theory of the icosahedral alloys in which some strain or defects or both have been frozen into the structure during solidification. Strains and defects are necessary to explain subtle deviations between the observed diffraction patterns of the icosahedral alloys and the diffraction patterns computed from ideal, icosahedral quasicrystals. Coincidentally, strong theoretical arguments have been developed that state that a particular type of strain, phason strain, relaxes very slowly in quasicrystals, and hence should be the dominant type of defect quenched during the growth of quasicrystalline solids. The strains and defects observed in the icosahedral alloys display the experimental signature of phason strain predicted by the theory.

In contrast, the experimental data are inconsistent with the straightforward versions of the multiple twinning and icosahedral glass models. No explicit model of either the multiple twinning or the icosahedral glass model exists that is consistent with all experimental data. One can imagine variations or elaborations of these two models or the large unit cell model that will lead to closer agreement with experiment (for example, the further increase in size of the unit cell or the addition of yet more packing constraints). However, with this approach, such models become increasingly artificial or, in some

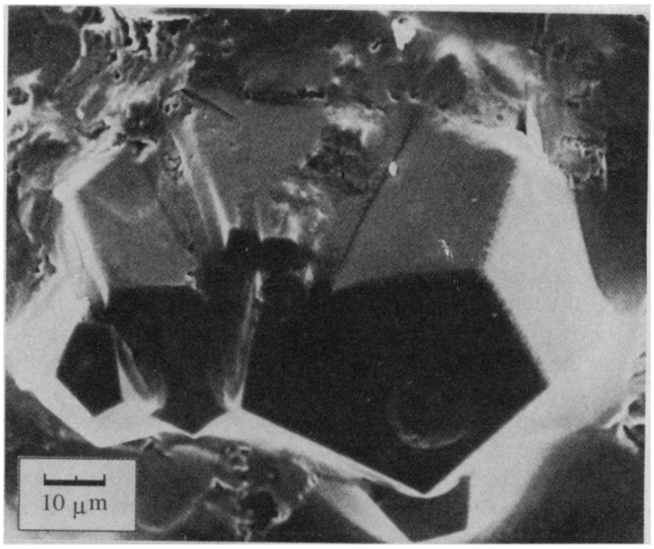

Fig. 5. A dendrite, approximately 100 μm across, of $GaMg_{2.1}Zn_{3.0}$ with flat facets oriented parallel to the faces of a pentagonal dodecahedron, the polyhedron that is dual to an icosahedron (that is, has the same rotational symmetry) [courtesy of F. Spaepen] (*23*). The facets are direct support for the icosahedral symmetry and long-range positional order predicted when the quasicrystal model is used.

cases, indistinguishable from the quasicrystal model and thus lose their distinctive predictive value (*7*).

Although the nature of long-range order is the fundamental issue addressed in this article, its resolution is only one of many challenges in the field. The quasicrystal model predicts the long-range atomic order in the icosahedral alloys, but the detailed locations of the atoms in the structure need to be determined (*9*). The ultimate challenge, however, and the focus of present research in the field is to determine the structural, thermal, and electronic properties that characterize the new phase of matter (*8*).

REFERENCES AND NOTES

1. D. Shechtman, I. Blech, D. Gratias, J. W. Cahn, *Phys. Rev. Lett.* **53**, 1951 (1984).
2. D. Levine and P. J. Steinhardt, *ibid.*, p. 2477.
3. For a popular review of quasicrystals, see P. J. Steinhardt, *Am. Sci.* **74**, 586 (1986).
4. D. Shechtman and I. Blech, *Metall. Trans.* **16A**, 1005 (1985).
5. P. W. Stephens and A. I. Goldman, *Phys. Rev. Lett.* **56**, 1168 (1986); *ibid.* **57**, 2331 (1986).
6. L. Pauling, *Nature (London)* **317**, 512 (1985); *Phys. Rev. Lett.* **58**, 365 (1987).
7. The term "icosahedral glass model" has come to have different meanings to different scientists. Some scientists use the term "icosahedral glass model" to refer to icosahedrally symmetric solids with quenched positional disorder, independent of whether it comes from a well-defined microscopic packing rule. This allows for a continuum of possible structures, including a quasicrystal with quenched phason strains. With such a broad definition, the distinction between icosahedral glasses and quasicrystals is totally semantic. For this article, though, the term is used in the sense intended by P. W. Stephens and A. I. Goldman (*5*), who coined the expression, and by researchers who have constructed candidate models; that is, to refer to models in which positional disorder is introduced as a result of a fundamental interaction between microscopic clusters that results in a random packing rule. (I include the possibility of packing rules that differ from those already published in the literature.) In this case, there is a legitimate scientific distinction between the two models. The disorder produced by random packing rules takes a specific form that has a well-defined experimental signature and that is generally quite different from the predictions for quasicrystals, as is outlined in this article.
8. For an introduction and review, see P. J. Steinhardt and S. Ostlund, *The Physics of Quasicrystals* (World Scientific, Singapore, 1987), chap. 4.
9. C. L. Henley, *Comments Condensed Matter Phys.* **13**, 59 (1987).
10. R. Penrose, *Inst. Math. Appl. Bull.* **10**, 266 (1974).
11. V. Elser, in *Proceedings of the XVth International Colloquium on Group Theoretical Methods in Physics*, R. Gilmore and D. H. Feng, Eds. (World Scientific, Singapore, 1987).
12. See Scientific Correspondence, *Nature (London)* **319**, 102 (1986).
13. Issue on the International Workshop on Aperiodic Crystals, D. Gratias and L. Michel, Eds., *J. Phys. (Paris)* **47** (C3) (1986).
14. P. A. Bancel, P. A. Heiney, P. W. Stephens, A. I. Goldman, P. M. Horn, *Phys. Rev. Lett.* **54**, 2422 (1985).
15. P. A. Bancel and P. A. Heiney, *ibid.*, in press; J. D. Budai *et al.*, *ibid.* **58**, 2304 (1987).
16. T. C. Lubensky, J. E. S. Socolar, P. J. Steinhardt, P. A. Bancel, P. A. Heiney, *ibid.* **57**, 1440 (1986).
17. For a review and references on elasticity theory for quasicrystals, see T. C. Lubensky, in *Aperiodic Crystals*, M. V. Jaric, Ed. (Academic Press, Boston, in press).
18. W. Malzfeldt *et al.*, *J. Phys. (Paris)* **47** (C3), 379 (1986).
19. J. E. S. Socolar and D. C. Wright, *Phys. Rev. Lett.* **59**, 221 (1987).
20. P. J. Steinhardt, *ibid.* **57**, 2769 (1986); P. W. Stephens and A. I. Goldman, *ibid.*, p. 2270.
21. B. Dubost, J.-M. Lang, M. Tanaka, P. Sainfort, M. Audier, *Nature (London)* **324**, 48 (1986).
22. E. R. Ryba, *Earth Miner. Sci.* **55**, 51 (1986).
23. W. Ohashi and F. Spaepen, unpublished results.
24. A. R. Kortan, H. S. Chen, J. Waszczak, *J. Mater. Res.* **2**, 294 (1987).
25. P. M. Horn *et al.*, unpublished results.
26. S. J. Poon *et al.*, unpublished results.
27. Y. Shen *et al.*, *Phys. Rev. Lett.* **58**, 1440 (1987).
28. A. Garg and D. Levine, unpublished results.
29. I thank P. A. Heiney, J. E. S. Socolar, T. C. Lubensky, and D. C. Wright for discussions and for reviewing the manuscript, P. A. Bancel for providing Fig. 1, P. Horn for providing Fig. 4, and F. Spaepen for providing Fig. 5. This work has been supported in part by the National Science Foundation, Materials Research Laboratory Program, under grant DMR-8519059.

Research Articles

Purification and Properties of *Drosophila* Heat Shock Activator Protein

CARL WU, SUSAN WILSON, BARBARA WALKER, IGOR DAWID,
THOMAS PAISLEY,* VINCENZO ZIMARINO, HITOSHI UEDA

Drosophila **heat shock activator protein, a rare trans-acting factor which is induced upon heat shock to bind specifically to the heat shock regulatory sequence in vivo, has been purified from shocked cells to more than 95 percent homogeneity by sequence-specific duplex oligonucleotide affinity chromatography. The purified protein has a relative molecular mass of 110 kilodaltons, binds to the regulatory sequence with great affinity and specificity, and strongly stimulates transcription of the** ***Drosophila hsp70*** **gene. Studies with this regulatory protein should lead to an understanding of the biochemical pathway underlying the heat shock phenomenon.**

THE HEAT SHOCK RESPONSE WAS ORIGINALLY DISCOVERED in *Drosophila* (*1*) as the coordinate activation of a small number of cytogenetic loci in response to heat or chemical shock; it is now extensively studied as an evolutionarily conserved response to stress in all living species (*2*). The molecular analysis of heat shock gene activation has been advanced by genetic and biochemical approaches. Deletion mapping studies of the transcriptional regulation of these genes have identified a cis-acting heat shock control element (HSE), whose consensus sequence is CT-GAA--TTC-AG (*3*); sequences matching this heat-shock consensus sequence (HSC) are found in one or several copies upstream of the transcriptional start site.

Studies in our laboratory of protein-DNA interactions in vivo have identified a trans-acting factor referred to as heat shock activator protein (*4*), which is induced to bind specifically to the HSE only upon heat shock stimulation. HSE's of the noninduced genes are free of the protein and lie within nuclease hypersensitive sites in chromatin near the 5′ termini of these genes (*4, 5*). Heat shock activator protein can be extracted from nuclei of heat shock–

C. Wu, S. Wilson, B. Walker, T. Paisley, V. Zimarino, and H. Ueda are in the Laboratory of Biochemistry, National Cancer Institute, National Institutes of Health, Bethesda, MD 20892. I. Dawid is in the Laboratory of Molecular Genetics, National Institute of Child Health and Human Development, National Institutes of Health, Bethesda, MD 20892.

*Present address: Medical College of Virginia, Richmond, VA 23298.